Chapter 17

Analysis of Mitochondrial pH and Ion Concentrations

Martin vandeVen, Corina Balut, Szilvia Baron, Ilse Smets, Paul Steels, and Marcel Ameloot

Abstract

Detailed practical information is provided with emphasis on mapping cytosolic and mitochondrial pH, mitochondrial Na^+, and briefly also aspects related to mitochondrial Ca^{2+} measurements in living cells, as grown on (un)coated glass coverslips. This chapter lists (laser scanning confocal) microscope instrumentation and setup requirements for proper imaging conditions, cell holders, and an easy-to-use incubator stage. For the daily routine of preparing buffer and calibration solutions, extensive annotated protocols are provided. In addition, detailed measurement and image analysis protocols are given to routinely obtain optimum results with confidence, while avoiding a number of typical pitfalls.

Key words: Renal epithelial cells, MDCK, mitochondrial pH, cytosolic pH, mitochondrial sodium, mitochondrial calcium, SNARF-1, CoroNa Red, rhod 2, confocal microscopy.

1. Introduction

1.1. Scope of this Chapter

It is known that the transport function and fate of renal tubular cells are determined by the degree of ATP depletion (1), which will lead to a gradual increase in free cytosolic Ca^{2+}, due to the disturbance of ATP-dependent ion channels and the loss of activity of Ca^{2+}- and Na^+/K^+-ATPases. This will induce an activation of proteases and phospholipases, and will result in a progressive loss of cytoplasmic membrane integrity and eventually collapse of the cell. Prevention of increased Ca^{2+} influx in the renal tubular

The authors Martin vandeVen and Corina Balut have equally contributed

D.B. Papkovsky (ed.), *Live Cell Imaging*, Methods in Molecular Biology 591,
DOI 10.1007/978-1-60761-404-3_17, © Humana Press, a part of Springer Science+Business Media, LLC 2010

cells or mitochondrial sequestration will delay the onset of cell injury (2). Therefore we were interested in studying how mitochondria could buffer elevations in cytosolic Ca^{2+} in the presence of a disturbed cytosolic sodium and pH homeostasis. We used a culture of Madin–Darby canine kidney (MDCK) cells, inflicted with metabolic inhibition (MI) and assessed cytosolic and mitochondrial pH, and mitochondrial sodium and calcium concentrations. The results of these investigations have been reported elsewhere (3–5).

In this chapter we treat subsequently the protocols employed by our group to measure in living MDCK cells: (1) mitochondrial and cytosolic pH by dual emission confocal microscopy of carboxy SNARF-1; (2) mitochondrial Na^+ concentrations using CoroNa Red; (3) mitochondrial Ca^{2+} concentrations using rhod 2.

Methods and protocols as presented, take cellular and mitochondrial motility into account and may be applicable with some optimization to other cell types that adhere to glass coverslips, provided that the dyes can be loaded predominantly into the proper target cellular compartments. Our protocols can most likely not be applied to, for example, heart muscle cells since the number and density of mitochondria precludes the location of cytosol volumes free of contamination with mitochondrial signal.

1.2. Rationale Behind Choice and Properties of Fluorophore Dyes

1.2.1. MitoTracker Green Mitochondrial Stain

MitoTracker Green (MTG) is used to visualize the mitochondrial network. This is a cell-permeant dye, well retained by mitochondria at any mitochondrial membrane potential ($\Delta\Psi_m$). In methanol, its absorption maximum is close to the 488 nm laser line with an emission peaking near 515 nm, allowing the use of fluorescein filter sets. The dye is bright and allows mitochondrial imaging for extended periods of time when exposure to laser light is not too excessive (typically 10 μW at 488 nm and at the sample position).

1.2.2. SNARF-1 pH Indicator Dye

The methodology employed by our laboratory to measure the pH changes in the cytosol (pH_i) and mitochondria (pH_m) of living MDCK cells relies on using the pH-sensitive fluorophore 5-(and 6-)carboxy SNARF-1 (SNARF-1).

SNARF-1 is a fluorescent dye with a pK_a of approximately 7.3 at 37°C. This dual emission probe exhibits a large emission spectral shift in response to pH changes, making it suitable for monitoring pH_i and pH_m in living cells in the range of 6.8–7.8.

SNARF-1 is loaded into the cells as an acetoxymethyl ester (AM) analog, which is readily permeable to cell membranes (6). The ultimate intracellular distribution of the dye is dependent

on the activity of cytosolic and organelle esterases relative to the rate of uptake of the AM form of the dye into the cellular compartments. Post-incubation of SNARF-1 loaded cells for 2.5–3 h results in the accumulation of the dye into the mitochondrial compartment (7).

When excited at 568 nm, SNARF-1 demonstrates an isosbestic point at 585 nm and pH-dependent changes in emission intensity at 640 nm. Estimation of pH from the ratio of emission intensities at the two wavelengths has the advantage to correct for shortcomings such as photobleaching and leakage of the dye. Photobleaching appeared fairly strong for this dye loaded into MDCK cells. Limitation of the total exposure time to approximately 10 min is one of the aspects of the protocols listed.

1.2.3. CoroNa Red Na^+ Concentration Indicator Dye

Mitochondrial Na^+ concentrations ($[Na^+]_m$) can be monitored with CoroNa Red, a bright cationic dye that can be directly loaded into cells without using an AM ester precursor. Cellular uptake is rapid and produces predominantly mitochondrial localization (4). The dye has a good photostability as the fluorescence intensity decreases only about 1–3% after 30 times illumination. Since many physiological processes may involve the decrease of the $\Delta\Psi_m$ (e.g., ischemia), it is important to verify that even in extreme conditions the cationic CoroNa Red dye is retained in the mitochondrial matrix. Experiments using the mitochondrial uncoupler carbonyl-cyanide-4-(trifluoromethoxy)-phenylhydrazone (FCCP) prove that changes in $\Delta\Psi_m$ did not affect substantially the mitochondrial retention of CoroNa Red (4).

The spectral properties allow simultaneous imaging in the presence of MTG. Absorption and emission maxima occur at 554 and 578 nm. This allows for excitation with the 543 nm Green He-Ne laser line and detection with standard emission filters suitable for tetramethylrhodamine (TRITC).

The probe does not possess ratiometric properties preferred for easy correction and elimination of systematic errors. For MDCK cells the protocols were adjusted such that image series could be collected without an overwhelming influence of photobleaching.

1.2.4. Rhod 2 Ca^{2+} Concentration Indicator Dye

Mitochondrial Ca^{2+} concentrations ($[Ca^{2+}]_m$) can be monitored with rhod 2. The AM form is required for loading cells. Rhod 2-AM carries a delocalized positive charge and is readily taken up into polarized mitochondria. Upon hydrolysis of the ester moieties, the rhod 2-free acid remains trapped inside the mitochondria. An increase in $[Ca^{2+}]_m$ is reported by an increase in fluorescence intensity. Its spectral properties, excitation maximum at 540 nm and emission peak around 575 nm, allow imaging in the presence of the green MTG emitter dye. As rhod 2 is a strongly

bleaching dye, we had to limit in our protocols the total exposure time to approximately 5 min. For more information about these dyes consult the website of the rhod 2 supplier Invitrogen: http://www.invitrogen.com/.

1.3. General Measurement Strategy

The basic protocol for measuring mitochondrial pH, Na^+, and Ca^{2+} concentrations involves the following general steps: cells are trypsinized and then plated onto glass coverslips and allowed to reach 100% confluency under cell-type required conditions. Next, cells are simultaneously loaded with the ion sensitive fluorophore of interest (e.g., SNARF-1, CoroNa Red, or rhod 2) and the ion insensitive mitochondrial stain MTG. This double labeling allows discrimination between cytosolic and mitochondrial pixels, and avoids challenges due to mitochondrial or cell motility. The glass coverslip containing the cell monolayer is mounted in a holder and visualized on the stage of an inverted confocal microscope. The images in the MTG and the ion sensitive indicator channels are recorded under conditions that ensure the minimization of dye bleaching and a good signal–to-noise ratio. The mitochondrial and cytosolic regions of interest are carefully selected using a "MTG masking" procedure. The fluorescence recordings are calibrated to reflect the ion concentrations of interest. Corrections for autofluorescence, emission detection channel cross talk, acquisition bleaching, and detector linearity are required to ensure the reliability of the data.

In **Sections 2** and **3**, we list required ingredients for cell and tissue culture growth and measurement media, cell support preparation, the various buffer solutions, and their preparation methods with caveats as to their practical use. Instrumentation and measurement protocol issues to consider for proper imaging are provided in detail to make reliable data collection feasible even for the novice user.

2. Materials

2.1. Cell Culture

2.1.1. Coverslip-Related Material

1. 24-mm no. 1.5 round glass coverslips (Menzel-Gläser, Braunschweig, Germany).
2. 100% analytic quality Normapur absolute ethanol (VWR Intl., Leuven, Belgium).
3. Forceps.
4. 6-well tissue culture plates.
5. Optionally, poly-L-lysine (Sigma), depending on cell type and support.

2.1.2. Cell Culture and Medium

1. Cells of interest, growing in cell culture. We have used MDCK cells intermediate between type I and type II (ohmic resistance of 400–500 Ωcm^2 (8)), low passage 23–27, kindly provided by Dr. H. De Smedt, Laboratory of Molecular and Cellular Signalling, KULeuven, Belgium.
2. Cell culture medium. For MDCK cells use a 1:1 mixture of DMEM and Ham's F-12 (Sigma or Gibco), supplemented with 10% fetal calf serum (Sigma-Aldrich), 14 mM L-glutamine, 25 mM $NaHCO_3$, 100 U/ml penicillin, and 100 μg/ml streptomycin (Sigma). Store in the dark at 4°C.
3. Cell-culture-grade trypsin 0.05% trypsin–EDTA solution (Sigma). Store as 2–3 ml aliquots in the freezer.
4. Sterile phosphate-buffered saline solution (PBS), pH 7.4.
5. Light microscope with 10× and 20× objectives for cell inspection and counting.
6. Humidified incubator at 37°C supplemented with 5% CO_2.

2.2. Fluorophores

1. MitoTracker Green (Invitrogen): 400 μM stock solution in dimethyl-sulfoxide (DMSO).
2. 5-(and 6-)carboxy SNARF-1 acetoxymethyl (AM) ester acetate (Invitrogen): 5 mM stock solution in DMSO.
3. CoroNa Red (Invitrogen): 1 mM stock solution in DMSO.
4. Rhod 2-AM (Invitrogen): 1 mM stock solution in DMSO.
5. For Na^+ and Ca^{2+} measurements Pluronic F-127 (Invitrogen) (0.025% (w/v) from 25% (w/v) stock solution in DMSO) was used to facilitate the solubilization of the dyes.
6. All fluorophores stored in darkness at –20°C are stable for months (*see* **Note 1**).
7. Use aliquot stock solutions to avoid repeated freeze–thaw cycles. Prepare the stock solutions and the aliquots under the hood, using sterile pipette tips and eppendorf tubes, to avoid any contamination of the samples. When preparing the aliquots, keep the stock solution tube wrapped in aluminium foil to prevent prolonged light exposure (*see* **Note 2** for preventing contamination of DMSO with water).

2.3. Solutions and Chemicals

2.3.1. Normal Saline Solution (NSS)

140 mM NaCl, 5 mM KCl, 1.5 mM $CaCl_2$, 1 mM $MgSO_4$, 10 mM HEPES, and 5.5 mM glucose (pH adjusted to 7.4 with Tris, at 37°C). HEPES and Tris buffer prevent pH alteration due to CO_2. Store solution at 4°C in the dark (*see* **Notes 3–5**).

2.3.2. pH Calibration Solution

1. High-K^+ buffer: 145 mM KCl, 1.5 mM $CaCl_2$, 1 mM $MgSO_4$, 10 mM HEPES, and 5.5 mM glucose.

2. Nigericin (Sigma) stock solution: 13 mM in ethanol (to equilibrate the pH gradient across the plasma membrane).
3. Carbonyl-cyanide-4-(trifluoromethoxy)-phenylhydrazone (FCCP, Sigma-Aldrich) stock solution: 10 mM in ethanol (to equilibrate pH gradients across the mitochondrial membrane).
4. Oligomycin (mixture of types A, B, C) (Sigma) stock solution: 5 mg/ml in ethanol (to inhibit the mitochondrial H^+-ATPase).

2.3.3. Na^+ Calibration Solutions

1. Solution 145 mM Na^+ (30 mM NaCl and 115 mM Na-gluconate) and no K^+.
2. Solution 145 mM K^+ (30 mM KCl and 115 mM K-gluconate) and no Na^+.
3. Both calibration solutions also contain 1.5 mM $CaCl_2$, 1 mM $MgSO_4$, 10 mM HEPES, and 5.5 mM glucose. pH is adjusted to 7.4 with Tris. Store all solutions at 4°C.
4. Gramicidin D (Sigma): 2 mM stock solution in ethanol (to equilibrate the Na^+ gradient across the plasma membrane).
5. Nigericin (Sigma): 13 mM stock solution in ethanol.
6. Monensin (Tocris): 10 mM stock in ethanol (to equilibrate Na^+ gradients across the mitochondrial membrane).
7. FCCP: 1 mM stock solution in DMSO.
8. Oligomycin (Tocris, Bristol, UK): 5 mg/ml stock in ethanol.
9. Store nigericin, FCCP, gramicidin, and monensin stock solutions at 4°C. The oligomycin stock solution should be stored as aliquots at –20°C.

3. Methods

3.1. Cell Culture

3.1.1. Coverslip Preparation

1. In a tissue culture hood, under sterile conditions, soak the coverslips in ethanol possessing a very low autofluorescence and briefly flame them, to remove any drops of ethanol. Place the sterilized coverslips in a 6-well plate.
2. For cells that do not adhere very well on glass, the coverslip surface should be treated with poly-L-lysine: cover each sterilized coverslip with several drops of 1× poly-L-lysine solution and place the dish in the incubator at 37°C for 15 min. Next, place the dish in the tissue culture hood, using the overhead ultraviolet lamps, for another 15 min. Wash twice with sterile PBS.

3.1.2. Cell Culture Preparation

1. MDCK cells are maintained in a humidified 5% CO_2 atmosphere at 37°C. The growth medium is renewed every 3–4 days.
2. Deplate and split apart the cells by trypsinolysis (or the splitting method appropriate for that cell type). Add 2–3 ml 0.05% trypsin–EDTA for 10 min typically.
3. Collect floating cells. Centrifuge and resuspend in medium.
4. Perform the cell counting in order to plate the cells on the coverslips at a density of $0.5–2 \times 10^5$ cells/coverslip for pH, Na^+, and Ca^{2+} imaging. The droplet containing the cells has to be spread on the coverslip during the seeding, to have an equal distribution of cells over the whole coverslip.
5. Place the 6-well plates containing the seeded coverslips in the incubator (37°C, 5% CO_2) and use them after 3–5 days of culturing as follows: on the third day the monolayers seeded at 2×10^5 cells/coverslip; on the fourth and fifth day the monolayers seeded at 1×10^5 cells and 0.5×10^5 cells/coverslip, respectively. The moment of harvesting is determined by regular visual inspection on a sterile microscope stage under low magnification and looking for monolayer confluency without any dome formation (**Fig. 17.1**). Cell growth rate depends on cell type and passage number (*see* **Notes 6** and **7** on seeding density and passage number and **Note 8** on checking for mycoplasma contamination).

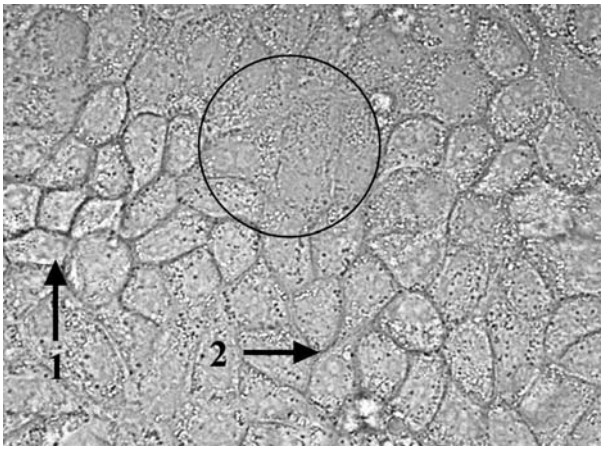

Fig. 17.1. Passage of MDCK cells after 5 days of growing (37°C, 5% CO_2). Changes in the monolayer morphology due to changes in the transport properties of the cells. Areas with cells forming domes (arrow 1) and patches of rounded cells (arrow 2) should be avoided during the measurement. Typically confluent areas, well attached to the glass are preferred for imaging (circled cells). Images collected with a Zeiss LSM 510 META confocal laser scanning microscope with 63×/oil objective, zoom 1, image size: 108.14 μm × 146.25 μm.

3.2. Cell Coverslip Holder and Imaging Hardware Material

1. Standard one-photon Zeiss LSM 510 META confocal laser scanning microscope (CLSM) with analog detection attached to an Axiovert 200 M frame (Zeiss, Jena, Germany), or equivalent.
2. Select 63×/1.4 Plan Apochromat oil-immersion objective or similar, with a suitable objective heater (PeCon GmbH, Erbach, Germany). This is meant to minimize the temperature differences between sample and objective, which otherwise impede image quality.
3. Install incubator adapted for the microscope stage, to maintain the cells at 37°C during the imaging. Our microscope is equipped with a model P type S (small) heated specimen holder with type S incubator (PeCon GmbH, Erbach-Bach, Germany) (*see* **Fig. 17.2c**).
4. Prepare holder and mount the glass coverslip covered with a nice confluent cell layer as checked with a standard transmission microscope image. We have used a homemade holder, but commercially available models are provided by most of the manufacturers of imaging systems. A layout of the in-house holder we have used is shown in **Fig. 17.2a and** an illustration of the complete assembly showing the plastic insert spacer with rubber seal and stainless-steel clamping cap is given in **Fig. 17.2b**. **Figure 17.2c** shows the assembly inside a small incubator mounted on top of the confocal stage.

Fig. 17.2. (a) Exploded view of the homemade cell holder with plastic spacer clamp and screw-on cap. (b) Completely assembled unit showing the plastic insert spacer with rubber seal and stainless-steel clamping ring. (c) Cell holder unit mounted inside PeCon GmbH heated incubator stage with warmed air overflow for 37°C verified sample temperature. Rear left of small incubator: Pt temperature sensor feedback. 63×/1.4 oil objective is also heated with a heating coil to minimize temperature differences between cells and environment. Device base diameter (bar) 58 mm, assembled height 15 mm (b).

3.3. Loading Protocols

3.3.1. SNARF-1 and MTG Loading for pH_i and pH_m Measurements

1. This procedure is to be performed immediately prior to pH_i and pH_m measurements. Serum contains esterases that may cleave the AM groups on SNARF-1. Therefore, all steps of the loading procedure should be carried out in serum-free medium. We have chosen to perform the loading in NSS.

2. Monolayers should be simultaneously loaded with SNARF-1 and the mitochondrial stain MTG. This allows during the processing step to discriminate between cytosolic and mitochondrial SNARF-1 pixels, and to avoid challenges due to mitochondrial or cell motility. Two loading procedures were developed: *Protocol 1*, where mitochondria are predominantly stained and *Protocol 2*, where SNARF-1 is loaded into both mitochondria and cytosol.
3. *Protocol 1:* Pre-warm the NSS solution at 37°C. Gently wash cells two times with NSS, to remove any serum traces from the tissue. Add on top of the cells 1 ml of NSS containing 10 μM SNARF-1 and 200 nM MTG from the stock solutions. Allow 30 min incubation time for the dyes to be internalized. Next, wash the monolayers two times with 1 ml NSS, and incubate for 2.5 h in NSS, to allow for complete hydrolysis and preferential mitochondrial compartmentalization of the dye. At the end of the incubation time wash the cells two times with NSS. Mount the coverslip on the microscope holder (**Fig. 17.2**). Place 1 ml of fresh NSS on top of the cells. Cover the top of the holder with a transparent plastic dish to prevent untimely evaporation and proceed with imaging (*see* **Note 9** on cell washing protocol).
4. *Protocol 2:* Wash cells with NSS. Load the cells for 30 min with 1 ml of NSS containing 10 μM SNARF-1 and 200 nM MTG. Wash the monolayers with NSS and allow 1.5 h incubation period, then apply a second loading step with 5 μM SNARF-1 for 30 min. Wash off the dye and incubate the cells in fresh NSS for another 30 min to allow for hydrolysis of the dye into the cytosol. Perform a two times wash with NSS in between each loading step (*see* **Note 10**).
5. Perform all the loading and washing steps in the 6-well plate, under the tissue culture hood. For all the required incubation times, keep the cells at 37°C in 5% CO_2.
6. The result of the two loading protocols is illustrated in **Fig. 17.3**.

3.3.2. CoroNa Red and MTG Loading for Mitochondrial Na^+ Determination

Cells are washed with NSS, then incubated simultaneously with 200 nM MTG and 2 μM CoroNa Red in 1 ml of NSS that contained 0.025% wt/vol pluronic F-127 for 30 min at 37°C. Loading has to proceed in the dark or with a dim red roomlight in order to protect the fluorescence dyes from bleaching.

3.3.3. Rhod 2-AM and MTG Loading for Mitochondrial Ca^{2+} Measurements

1. Cells were washed gently with NSS twice. Loading of MDCK cells with MTG and rhod 2 occurred in two subsequent steps. At first, MTG (200 nM) was loaded into the cells for 30 min at 37°C. This was followed by incubation

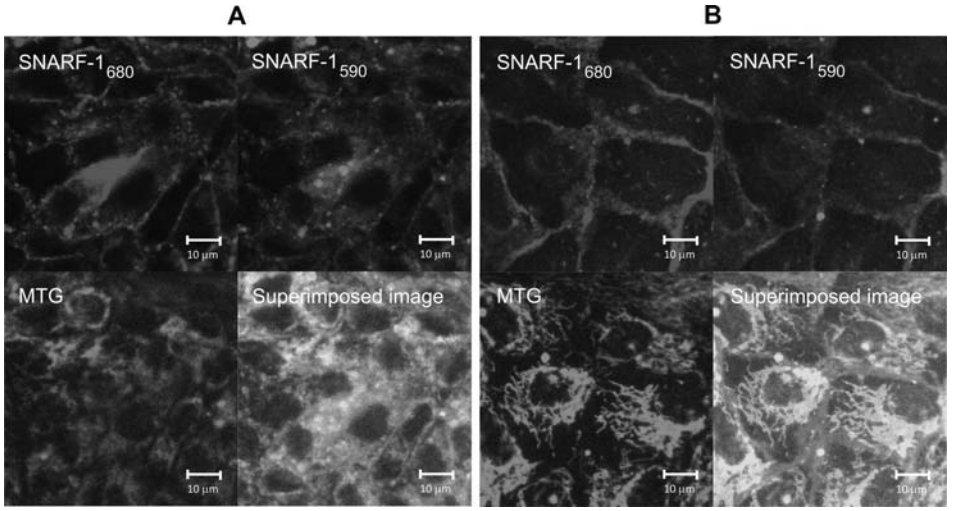

Fig. 17.3. Images of confluent monolayers of MDCK cells immediately after loading with both SNARF-1 and MitoTracker Green (MTG). Shown are emission detection channels for SNARF-1 (680 and 590 nm) and MTG (525 nm) according to two loading protocols: (**a**) Protocol 1; (**b**) Protocol 2 (for details see text). The superimposed images in each panel represent an overlay of the three others. The images in panels A and B were measured with identical settings of the confocal microscope. Reproduced with permission from *Kidney Int* (3).

of the cells for 30 min at 37°C in a loading solution containing rhod 2-AM (4 μM), MTG (200 nM), and pluronic acid (0.025% w/v) (5). Loading has to proceed in the dark or with a dim red roomlight.

2. Performing the loading procedure on the microscope stage, even in a standard atmosphere, offers the distinct advantage of imaging the background on exactly the same cells for later background subtraction. The buffer composition (HEPES and Tris) will maintain a constant pH independent of the presence of CO_2. For prolonged loading protocols like for SNARF-1 (3 h), it is better to maintain the cells in conditions that will ensure their normal physiological behavior.

3.4. Hints for Image Collection on Adherent Motile Cells

3.4.1. Optimization of Confocal Settings

1. The main tasks involve the following: (a) juggling the optimization of pinhole size, optical slice thickness for maximum detail and contrast; (b) minimizing fluorochrome bleaching and cellular stress. At the same time the cells and tissues have to stay in viable condition during imaging; (c) dealing with motile cells which may render automation of image processing protocols impractical and manual selection of regions of interest may become an arduous task; (d) obtaining workable signal and low background levels with a sustainable signal-to-noise ratio to numerically extract information from collected images.

2. Typical mitochondrial size is of the order of 200 nm. This is very close to the optical resolution of a microscope equipped with a 63×/1.4 oil objective. One may expect for 488 nm excitation and detection at 520 nm a radius for the Airy disk (influences the optical resolution) in the *xy* plane of 223 nm and in the Z-direction about three times worse: 669 nm. Reported values for the shape factor S (ratio of *z*-axis axial/*xy* plane radial Airy radius) may even be 5 or 7 and vary slightly from day to day. For 633-nm excitation with fluorescence emission observed at 650 nm these numbers relax about 25%. For maximum detail in living cells and tissues with excellent contrast, a small pinhole size is necessary. Even with minimal pinhole size (1 Airy), images of the mitochondrial network stay rather fuzzy even after deconvolution. Moreover, in the Z-direction the spatial nature of this network creates overlap. For studying mitochondria, an extended confluent layer of cells with a vast thin cytosol layer will make life easy.
3. When more than one detection channel is used, pinhole size has to be adjusted for each channel in order to have the same observed optical slice thickness for all emission channels. An emission channel consists of the collection of all optical elements, pinholes, lenses, optical filters, and detector. Using a confocal pinhole in front of the detector providing optical section capabilities to a microscope results in both stray-light and fluorescence reduction from layers not in focus, as well as an increase in image crispness. Look always for user-friendly features in CLSM software packages that will show the pinhole size and optical slice thickness directly in micrometers.
4. Photobleaching is always present and varies for each fluorochrome used. It is recommended to always perform pilot studies not only to optimize the loading protocol but also to evaluate the bleaching properties of the stains and changes in mitochondrial shape or levels of autofluorescence. For our measurements on MDCK cells, we had to decide to drastically minimize the number of exposures to laser light. Once the illumination protocol is optimized one can gain confidence in the validity of the collected images. With each new plating cycle the level of autofluorescence should be checked again for proper image correction. Damage caused by the illumination intensity will be somewhat relaxed when using a Nipkow type spinning disk which utilizes lamp illumination and parallel multiple pinholes of fixed diameter.
5. Both one- and two-photon illumination give rise to photochemical and photophysical effects, i.e., bleaching of fluorophores and photo-induced stress on cells. This stress will

show as a retraction and clustering of the mitochondrial network to the nuclear perimeter. In worse cases mitochondrial swelling may be observed with an increase in autofluorescence.

6. Practically the fluorescence signals may be very low (partially on purpose because of the minimal illumination to limit photobleaching) but should stay above the background signal level. Confocal microscope pinholes are usually NOT set to obtain diffraction-limited performance, but their settings should allow collection of images with a reasonable signal-to-noise ratio.
7. For our mitochondria images the "software derived" optical slice thickness was <2.4 μm. **Fig. 17.4c, d** show radial *xy* and axial *z*-direction point spread functions as measured on sub-resolution fixed 175-nm beads (Invitrogen, Merelbeke, Belgium) under experimental conditions as similar as possible with respect to the cell or tissue measurements. This apparently relatively poor resolution along the *z*-axis due to a rather extended detector pinhole size is a compromise in order to observe weak fluorescence with acceptable signal-to-noise ratio for extended periods of time.

3.4.2. Image Collection Settings

This section will present what settings one should use to image pH_i, pH_m, and mitochondrial ion concentrations in living MDCK cells on a standard one-photon Zeiss LSM 510 META CLSM or similar instrumentation. These settings, chosen to minimize bleaching and get a reasonable signal for the fluorophores used (listed in **Section 2.2**), should be tested and optimized if other cell types or confocal imaging systems are to be used.

1. Collect 512 × 512-pixel 8-bit (or 12 bit for better dynamic range) images, averaged twice (via software-selected repeated line scan mode) to improve the signal-to-noise ratio. A bit depth of 8 carries 256 gray values with black being zero and white being 255. In gray scale images pixel values below about 50 appear pitch black to the eye. It is very helpful during image collection and processing to switch to the Zeiss supplied Rainbow2 Look Up Table (LUT). With this LUT differences between a glass background and autofluorescence levels become easy to detect.
2. All Na^+ images were collected with a digital zoom factor of 1, while pH and Ca^{2+} images were collected with a digital zoom factor of 2. Pixel dwell time was always 25.6 μs.
3. MTG was excited by an Ar laser (488 nm line, 1% = 10 μW laser power at the sample position). SNARF-1, CoroNa Red and rhod 2 were excited with a Green HeNe laser (543 nm line, respectively 10 and 3.5% of 0.1 μW at the sample position).

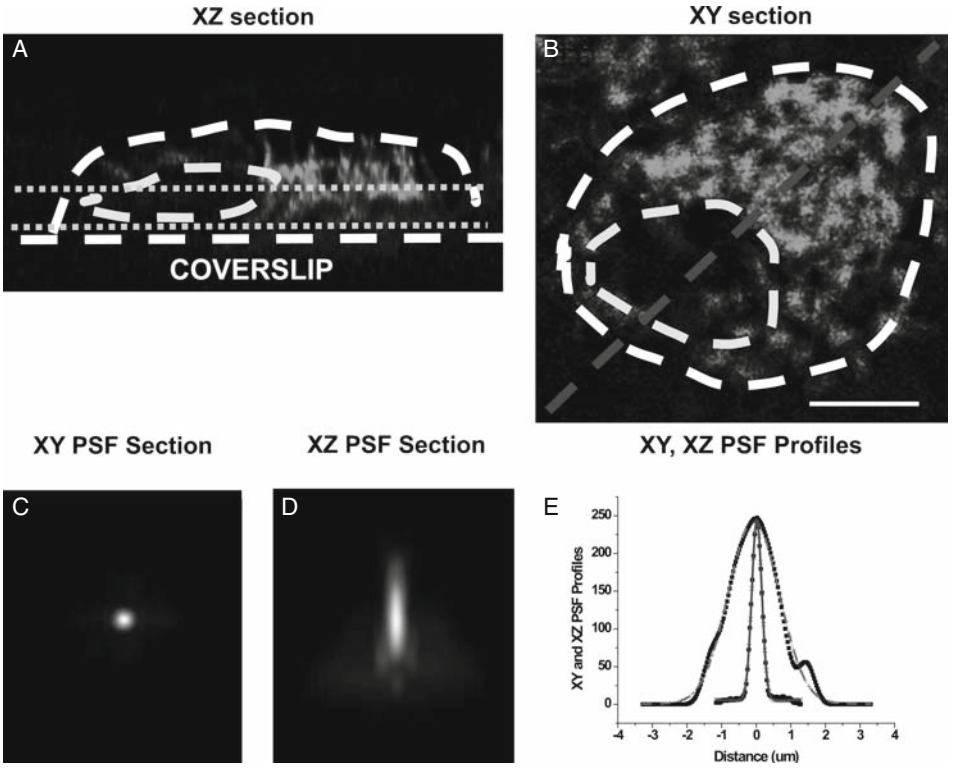

Fig. 17.4. Pixel selection in MDCK cells. Diagonal *xz* cross-section (**a**) and *xy* optical slice near support (**b**) as collected. Scale bar 10 μm. Image collection parameters: Zeiss 63×/1.4 oil plan-ApoChromat objective, zoom 2, pixel dwell time 6.4 μs, pinhole 325 μm for 488 nm excitation, 0.8% 488 nm excitation laser light with 10 μW on sample. Designation for the demarcation lines: *horizontal dotted lines* (**a**) – actual optical slice position with thickness to scale; external *circular dashed line* (**b**) – cell perimeter; inner *circular dash line* (**b**) – nucleus of MDCK cell; *diagonal grey dashed line* (**b**) – position of diagonal vertical cross-section. Cytosolic SNARF-1 signal retrieval in cells loaded according to Protocol 2: selection of pixels underneath the nucleus not having any discernable MTG contribution after digital signal enhancement. Mitochondrial SNARF-1 signal retrieval in cells loaded according to Protocol 1. Panels (**c**) and (**d**): *xy* and *xz* point spread function (PSF) cross-sections at 488 nm excitation for averaged unresolved microbead intensity images. Panel (**e**) horizontal (*xy*) $1/e^2$ width 0.56 μm, vertical (*xz*) $1/e^2$ full width 3.3 μm as obtained by Gaussian curve fit with $R^2 = 0.99$. Estimated error is 5%. *xz* for slice thickness (Zeiss software indicates slice thickness as < 2.4 μm). Theory predicts for the FWHM width of a diffraction-limited spot with 488 nm excitation 0.19 μm (*xy* plane) and 0.45 μm (*xz* plane). Reproduced with permission from *Kidney Int* (3).

4. SNARF-1 and rhod 2 are fast bleaching dyes, while CoroNa Red and MTG are very stable. Therefore, set the scanning sequence in such a way to capture first the fluorescence emission of the fastest bleaching dye, followed by the less bleaching one. For pH measurements: scan first SNARF-1 at 590 and 680 nm, through the 545 dichroic mirror with 565–615 and 655–705 nm bandpass (BP) filters, respectively. For $[Na^+]_m$ measurements: scan CoroNa Red via the 545 dichroic and 560 nm longpass (LP) filter. For $[Ca^{2+}]_m$ measurements: scan rhod 2 via the 545 dichroic and 590/25 nm BP filter. For all protocols, collect the MTG

signal the last, using a 490 dichroic and a 525/25 nm BP filter.

5. To minimize photobleaching and phototoxicity as much as possible while still maintaining discernable image detail toward the end of our experiments, laser power had to be kept as low as possible. At the same time, for pH imaging a 325-μm-diameter (~3 Airy units) pinhole setting had to be used for 488 nm and was adjusted accordingly for 543 nm excitation. This ensured an equal optical slice thickness of <2.4 μm (*see* **Note 11**). For Na^+ and Ca^{2+} measurements, the thickness of the optical slices was <1.4 μm for all experiments.
6. The detector gain should be optimized to avoid saturation in any pixel while maintaining a proper signal-to-background noise ratio. When measuring pH_m (cells loaded as in Protocol 1) and also mitochondrial Na^+ and Ca^+, the detector gain was always kept constant (e.g., 1100 for pH_m measurements). During the measurement of pH_i (cells loaded as in Protocol 2), the detector gain had to be adjusted between 800 and 1100 (Zeiss software settings) due to the rapid loss of dye from the cytosol. In this case, detector gain settings have to be separately calibrated (*see* **Section 3.4.3**).
7. For pH measurements: to facilitate the subsequent image analysis (see below), it is strongly recommended to choose the observation volume close to the basolateral membrane. In this way, the optical slice thickness enables part of the cytosol to be visualized underneath the nucleus region (**Fig. 17.4a**).

3.4.3. Required Image Intensity Corrections

Typical image intensity corrections include removal of the influence of autofluorescence, cross-talk between detection channels, effects of photobleaching, photomultiplier (PMT) detector linearity, and gain settings. SNARF-1 related pH image corrections serve as an example.

1. *Corrections for autofluorescence*. The autofluorescence levels should be measured on blank, unloaded cells, under similar experimental conditions and microscope settings as for the loaded cells. For blank cells, the pattern of mitochondrial areas and cytosolic areas underneath the nucleus appear clearly distinct in the SNARF-1 detection channels, allowing the background autofluorescence level to be measured for each compartment. Use Palette – Rainbow mode in the Zeiss LSM Image browser, to easily visualize the mitochondrial pattern of blank cells (**Fig. 17.5**). Use the image processing protocol as described in **Section 3.5.4** to calculate the background autofluorescence values related to the mitochondria and cytosol respectively. *See* **Note 12** on the importance of autofluorescence corrections, especially for

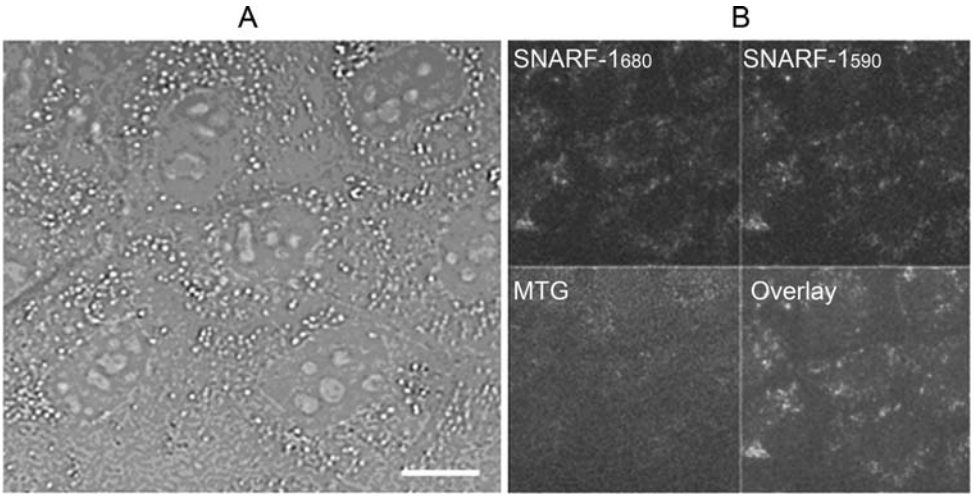

Fig. 17.5. Confluent monolayer of unlabeled MDCK cells, passage 25. (**a**) Transmission image; (**b**) background-signal on the three measured channels. All four panels display in gray-scale the Rainbow LUT provided by the Zeiss software. Cells were observed at detector gain 1100 (Zeiss software settings). Scale bar = 10 μm.

the pH protocol. In our measurements the mitochondrial background was consistently higher than the cytosolic background, although constant for the observed monolayers and individual passage numbers. Averaged values corresponding to mitochondria- and cytosol-related pixels were used to correct for the respective background signal. Glass coverslip background with buffer signal contributions can be estimated from areas free of any cells. Typically this background signal was 16–17 on an 8-bit (0–255) scale. Whenever the protocol requires the adjustment of the detector gain values during the measurement, the autofluorescence values corresponding to mitochondrial and cytosolic regions should be measured on blank cells at the respective detector gain values and used accordingly for background subtraction. **Figure 17.6** presents the changes in mitochondrial autofluorescence as a function of the detector gain, under our experimental conditions. Cytosolic autofluorescence was less sensitive to the changes in the detector gain, ranging between 17 and 20. Repeated exposure of cells to laser illumination may influence the level of autofluorescence of the cells and may prove to be phototoxic to them. In our experimental protocol, the autofluorescence proved to be constant over the duration of the experiment with identical illumination protocols, both for untreated control cells as well as for cells exposed to MI. Autofluorescence in CoroNa Red and rhod 2 images was always very small (*see* **Note 13** on published conditions to avoid phototoxicity).

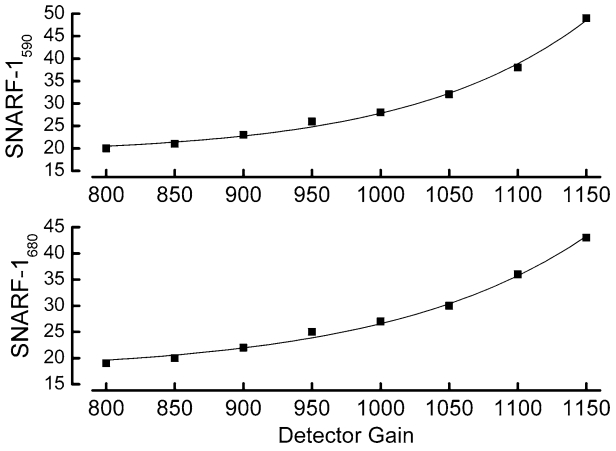

Fig. 17.6. Autofluorescence intensity (arbitrary units) of mitochondrial area as a function of detector gain values applied (Zeiss software settings) on each of the two SNARF-1 channels.

2. *Confocal laser scanning microscopy detection channel crosstalk.* To check for the crosstalk between the SNARF-1 and MTG channels, fluorescence should be measured in the corresponding channels for SNARF-1_{590}, SNARF-1_{680}, and MTG for monolayers loaded either only with SNARF-1 (following loading Protocol 1) or only with MTG. With the chosen settings, when SNARF-1 emission was measured in the MTG channel, only the autofluorescence signal was observed. Similarly, the MTG emission in the SNARF-1 channels only gave the basal background value, ensuring that there is no measurable crosstalk between the detection channels (**Fig. 17.7**). For the detection conditions as listed,

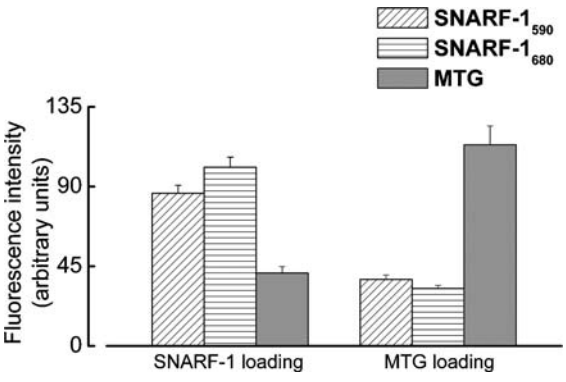

Fig. 17.7. Crosstalk check between the SNARF-1 and MTG channels. Fluorescence was measured in the corresponding channels for SNARF-1_{590}, SNARF-1_{680}, and MTG for monolayers loaded either only with SNARF-1 or only with MTG. Detector gain 1100 (Zeiss software settings). Values from four different monolayers are reported as mean ± SEM (standard error of the mean). Reproduced with permission from *Kidney Int* (3).

crosstalk was checked and found to be absent between MTG and CoroNa Red (Na^+) as well as rhod 2 (Ca^{2+}) and MTG detection channels.

3. *Photobleaching*. SNARF-1 and MTG bleaching should be checked on cells loaded separately with the individual dyes or when both were present. In our experimental protocol, MTG was never affected by bleaching. Data indicated pronounced bleaching of SNARF-1 during image sequence collection, but the SNARF-1 ratio (680 nm/590 nm) proved constant over time (**Fig. 17.8**). CoroNa Red was found to be very photostable, whereas rhod 2 rapidly bleached under our experimental conditions. Therefore the number of image collection events in rhod 2 loaded cells was restricted to four measurement points (*see* **Note 14**).
4. *Photomultiplier linearity*. To be able to see the weakened cytosolic SNARF-1 signals, PMT voltages should be adjusted and calibrated. PMT calibration was performed on

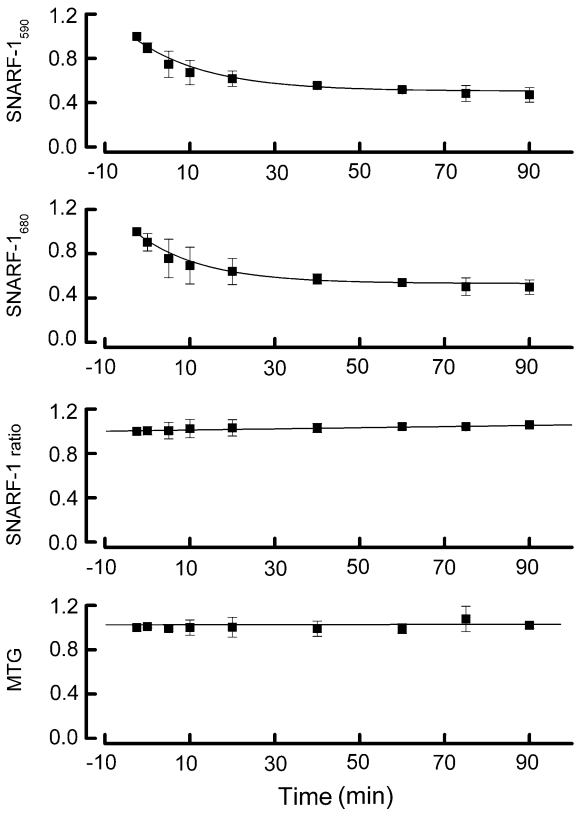

Fig. 17.8. Bleaching of SNARF-1 and MTG. Bleaching rates for SNARF-1_{590}, SNARF-1_{680}, Ratio SNARF-1_{680}/SNARF-1_{590}, and MTG measured under Protocol 1 loading conditions. Values are indicated as mean values ± SEM for two monolayers. Data are normalized in each case to the starting value to clearly show the trend over time. Reproduced with permission from *Kidney Int* (3).

cells loaded only with MTG, which showed no photobleaching for the conditions reported here. To obtain the calibration curve, the fluorescence in the MTG channel was recorded at different detector gain values in the range of 800–1100, while maintaining the same scanning parameters (laser intensities, pinhole, zoom, etc.) as presented in **Section 3.4.2**. An example of a typical calibration curve obtained is presented in **Fig. 17.9**. This PMT calibration was not important for CoroNa Red and rhod 2 experiments, since all images were detected with the same detector gain initially optimized to be in its linear response region.

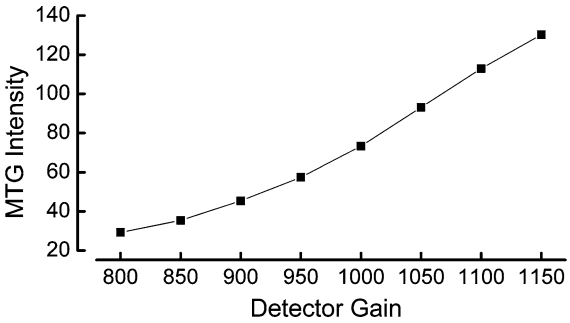

Fig. 17.9. Detector response and linearity as a function of detector gain applied (Zeiss software settings) as measured in the MTG channel.

3.5. Extracting Image Information

3.5.1. Software

For image transfer, conversion, and processing, the freeware Zeiss LSM Image Browser and ImageJ Java-based freeware (Research Services Branch, National Institute of Mental Health/National Institute of Neurological Disorders and Stroke, Bethesda, MD) plug-in routines were used. Excel (Microsoft Corp, Redmond, WA) and Origin (OriginLab Corp, Northhampton, MA) were used for statistical data analysis. Huygens Essential and the point distiller package (Scientific Volume Imaging, Hilversum, the Netherlands) was used for point spread function analysis.

3.5.2. Selection of Pixels Containing Mitochondrial pH Information Based on SNARF-1 and MTG Image Processing

1. Data collection. To avoid as much as possible contamination of the mitochondrial related pixels with cytosolic information, the mitochondrial SNARF-1 information was obtained from cells loaded with SNARF-1, according to Protocol 1. At each time point, a set of three sequential (hereafter called multi-track) images was collected under presented settings (**Section 3.4.2**).
2. Create stack images. Using the ImageJ LSM Toolbox plug-in (Dr. J. Mutterer et al., University of Strasbourg, France) or the Zeiss supplied export routine, convert raw confocal images to 8-bit TIFF files (TIFF = Tagged Image File Format, with extension .tif). Store the files corresponding

to each confocal channel, in a separate folder. Use number extensions to designate the time sequence of the files. In ImageJ use File→ Import to create a stack with the TIFF files measured on each confocal channel, for the entire experiment. Apply: Process → Noise → Despeckle. Save the despeckled stacks (e.g., SNARF590Stack.tif, SNARF680Stack.tif and MTGStack.tif) for subsequent analysis.

3. Eliminate saturated pixels by zeroing. Each of the stacks created for a certain experiment should be checked and corrected for any saturated pixels (occasionally present typically in the first image, since it was opted not to change standard detection settings once an experiment was under way). For this, open in ImageJ a Despeckled.tif stack. Go to Image → Adjust → Threshold. Set both low and high threshold sliders to the maximum pixel value: 255 (**Fig. 17.10a**). The saturated pixels will appear highlighted (arrows in **Fig. 17.10b**). Create the mask for saturated pixels: ImageJ→ Process → Binary → Make Binary. An image having all the saturated pixels 0 (black) and the remaining pixels 255 (white) will be created (**Fig. 17.10c**). Divide this image by the value 255, using Process → Math → Divide. This will create the mask image having all the saturated pixels zero (0) and the remaining desired ones with a value of one (1). Save this file (e.g., xxxxDespeckledSaturationMask.tif).

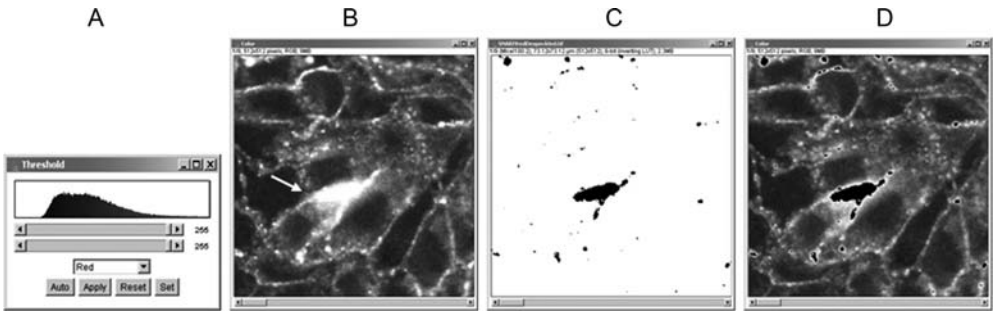

Fig. 17.10. The correction of saturated pixels exemplified on SNARF-1_{680} images. (**a**) Intensity histogram. (**b**) Highlighted saturated pixels (see *arrow*). (**c**) Mask image (255 = white and black = 0). (**d**) Saturation corrected image stack.

Multiply the original despeckled stack with the mask stack: Process → Image Calculator. The stack corrected for saturated pixels will be created in a new window (**Fig. 17.10d**). Save this file under a different name (e.g., xxxxDespeckled-SaturationCorrected.tif).

In the same way correct for any saturated pixels present in the other measured channels (SNARF-1_{590} and MTG).

4. Subtract background fluorescence. The background values corresponding to mitochondrial images should be

subtracted from SNARF-1_{680} and SNARF-1_{590} channels prior to any subsequent calculations. For this protocol, at the constant detector gain of 1100, the background values ranged between 37 and 38. The procedure for background values calculation is detailed in **Section 3.5.4**.

5. Create the MTG mask (*see* **Note 15**). MTG pixels related to a strong mitochondrial signal are selected by setting a high threshold. All pixel values in the MTG image between a variable lower limit (threshold value typically higher than 90–120) and the 255 maximum pixel value were used to create the mitochondrial mask. The careful pixel selection in the image analysis procedure allows obtaining mitochondrial SNARF-1 signals that are mainly of mitochondrial origin. The possibly few existing saturated pixels in the MTG image should be eliminated.

   After setting the threshold use Process → Binary → Make Binary. Then Process → Math → Divide by 255. This will create the MTG mask, having the mitochondria related pixels 1 and all the remaining ones 0. Save this file (e.g., MTGDespeckledMaskThres90.tif).

6. Mitochondrial SNARF-1_{680} and SNARF-1_{590} retrieval from MTG mask. Ratio calculation.

   Multiply the MTG mask with SNARF-1_{680} and SNARF-1_{590} stacks, respectively. Store the images in separate folders. To obtain the SNARF-1 ratio image, divide pixel by pixel the masked stacks SNARF-1_{680}/SNARF-1_{590}. Use: Process → Image Calculator → Divide (**Fig. 17.11**). Via Analyze → Measure, calculate the Ratio values corresponding to the entire stack. Save the result file as.txt for subsequent import in Excel or Origin and statistical analysis. pH_i and pH_m are expressed as the SNARF-1 (680 nm/590 nm) emission

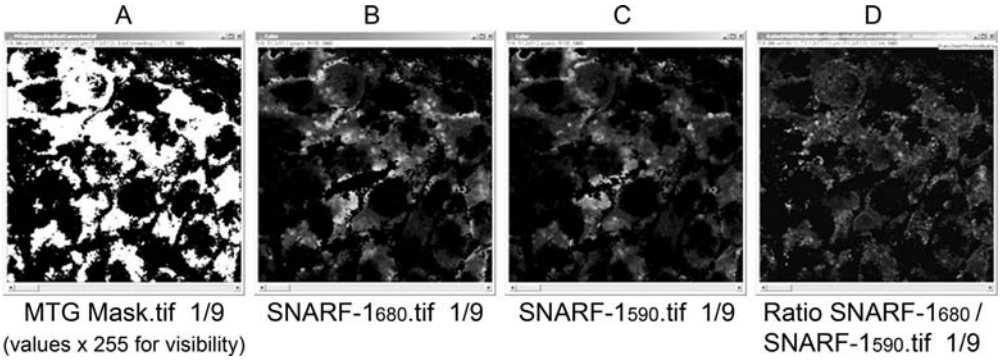

Fig. 17.11. MTG mask and retrieval of SNARF-1_{680}, SNARF-1_{590} mask images, and the ratio SNARF-1_{680}/SNARF-1_{590}. First image from a stack of nine is shown.

ratio. A decrease in the SNARF-1 ratio represents a decrease in pH.

3.5.3. Selection of Pixels Containing Cytosolic pH Information Based on SNARF-1 Analysis in the Volume Beneath the Nucleus

1. Data collection. Based on the observation that SNARF-1 is not staining the nucleus at all, and given that the cytosol underneath the nuclear area contains very few mitochondria (**Figs. 17.3 and 17.4**), the cytosolic SNARF-1 intensity was measured by choosing only the SNARF-1 related pixels in the cytosol underneath the nucleus (**Fig. 17.4**), for cells loaded following Protocol 2. As mentioned, the observation volume was always chosen close to the basolateral membrane, the optical slice thickness enabling part of the cytosol to be visualized underneath the nucleus region. Collect at each time point a set of three multi-track images (SNARF-1_{680}, SNARF-1_{590}, and MTG, respectively).
2. Create the corresponding stacks for each channel, with data converted to 8-bit TIFF files, despeckled and corrected for any saturated pixels, as presented above in **Section 3.5.2**.
3. Subtract the corresponding background values from each SNARF-1 stack. For cytosolic pixels under the nucleus, this value was always low (~18–20) and was determined as described in **Section 3.5.4**.
4. Selection of the cytosolic pixels under the nucleus. To select the proper cytosol related region of interest (ROI) underneath the nucleus, the MTG signal should be set to maximum contrast via digital image enhancement and histogram stretching using the image analysis software (**Fig. 17.12a**). This prevents accidentally selecting pixels with a hardly discernable weak MTG signal. Store the enhanced MTG stack in a different file (e.g., xxxxEnhanced.tif). Next, per individual MTG image, delineate for each cell the darkest nucleus area (no trace of MTG) using ImageJ → Polygon symbol. Store the selected pixels in a separate folder using File\Save As\Selection\Polygon11.roi, Polygon12.roi, Polygon13.roi, etc. Typically, 5–15 small circular, elliptical, and hand-drawn ROI regions were selected. Check whether the chosen ROIs have any bright cell wall pixels in the corresponding SNARF-1_{680} and SNARF-1_{590} images (**Fig. 17.12b and c**). If necessary, adjust the ROIs to avoid wall pixels and store the newly defined ROI under the same name (*see* **Note 16**). Under Analyze\Tools\ROI Manager open all ROIs belonging to an image in a stack and Combine them. This binds the Polygon ROIs to a single composite one, in order to be able to open for each image in SNARF-1_{680} and SNARF-1_{590} all via MTG selected nucleus area pixels.

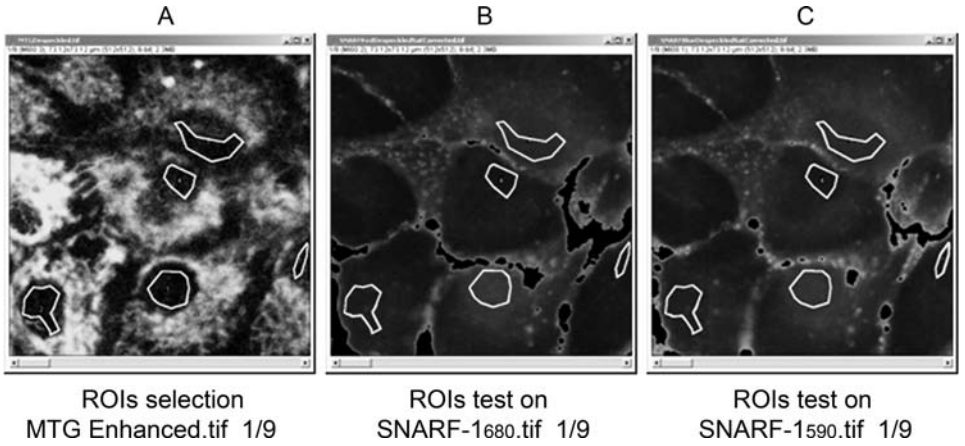

Fig. 17.12. Examples of the ROIs selection. First image of a stack of nine is shown. (**a**) MTG and (**b**) and (**c**) SNARF-1 images.

Repeat this procedure for all images in a MTG stack, starting again with the corresponding MTGEnhanced.tif file. It saves time to check whether the ROIs of the previous image (n–1) in the stack also fit the new MTG image, n, in the stack i.e., the cells did not move too much. When this is true, keeping the integrity of the Composite.roi, save Composite-n.roi. When, however, SNARF-1_{680} and SNARF-1_{590} show wall pixel overlap, the new Composite-n.roi has to be adjusted by changing the individual Polygon-(n–1).roi outlines.

5. Create the cytosolic pixels mask. Due to cell movement, it is necessary to create an individual cytosolic mask, based on the associated Composite.roi, for each image in the stack: in ImageJ create a new 8-bit TIFF file, then open the Composite-1.roi, for the first image in the stack. Invert and divide by 255. This will create an image having all the cytosol related pixels "1" (white) and the remaining ones "0" (black) (**Fig. 17.13**). Save as CytosolMask1.tif in a separate folder.

   Make in the same way, one by one, the CytosolMask-n.tif files, for the remainder of the images in the stack, using the associated Composite-n.roi.

   Bundle in a stack all the mask images, being careful to respect the correct sequence. Save in a separate file (e.g., CytosolMask.tif stack).

6. Cytosolic SNARF-1_{680} and SNARF-1_{590} retrieval from MTG mask and ratio calculation.

   Multiply the CytosolicMask.tif stack with SNARF-1_{680} and SNARF-1_{590} stacks, respectively. Store the images in separate folders. To obtain the SNARF-1 ratio image, divide

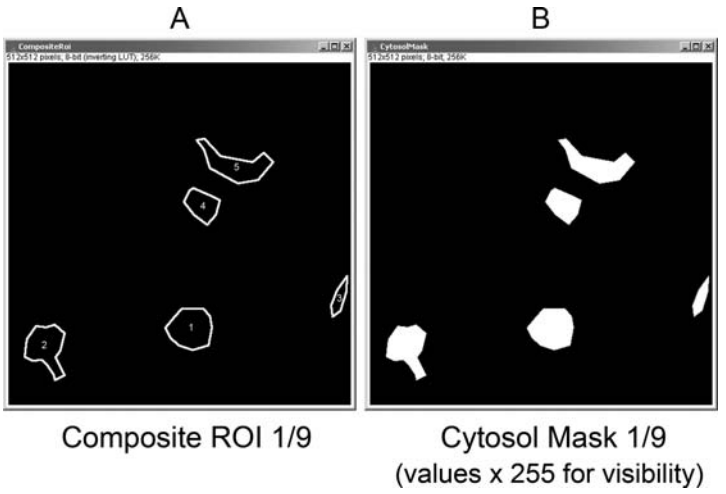

Fig. 17.13. (**a**) Example of a composite ROI for the first image out of a stack of nine. Each individual ROI in the composite image is numbered. This identification number allows retrieval of ROI statistics from the ROI export list feature in ImageJ; (**b**) cytosol areas free of any discernable MTG signal (*white* = 1) and area to be discarded (*black* = 0).

pixel by pixel the masked stacks SNARF-1_{680}/SNARF-1_{590}. Use: Process → Image Calculator → Divide. In Analyze → Measure, calculate the ratio values for each image in the stack. Save the result file as .txt for subsequent import in Excel or Origin and image statistics.

3.5.4. Estimation of Background Level for Mitochondrial and Cytosolic Areas on Blank Cells

This procedure is only required for the pH measurements protocol. It is not applied to the rhod 2 or the CoroNa Red experiments, which only use the brighter mitochondrial image regions outside the nucleus area.

After measuring the blank cells using the settings presented in **Section 3.4.2**, create the despeckled stacks from the images acquired for the three channels: SNARF-1_{680}, SNARF-1_{590}, and MTG.

1. Background values for mitochondrial pixels.
   Adjust via ImageJ the low threshold value, until the mitochondrial pattern becomes visible and well-defined dark nuclei areas are observed (**Fig. 17.14**). For our measurements, the low threshold value ranged between 20 and 30, depending on the value of detector gain during the measurement. Use Analyze → Measure and calculate the averaged values for the pixels related to mitochondria, at the selected threshold. Slide the image sequence cursor and calculate the corresponding values for all the images in a stack. Save the data as a .txt file. This will make it easier to import them into Excel or Origin for statistical analysis.

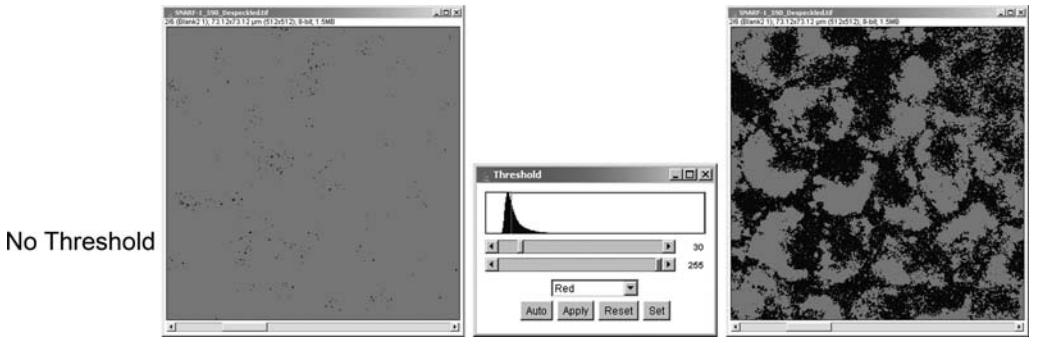

Fig. 17.14. Threshold selection to visualize the mitochondrial pattern on blank unstained cells.

2. Background for cytosolic pixels.
   To obtain the background values of the cytosol beneath the nucleus, apply the following sequence for both SNARF-1_{680} and SNARF-1_{590} stacks. Open stack, then enhance contrast, so all the bright areas related to mitochondria become clearly visible. Using the ROI manager in ImageJ, select small areas in the region of the nucleus, free of any discernable mitochondrial signal (**Fig. 17.15**). Combine all the ROIs selected for the first image in the stack in a composite image. Save it in a separate file, with the appropri-

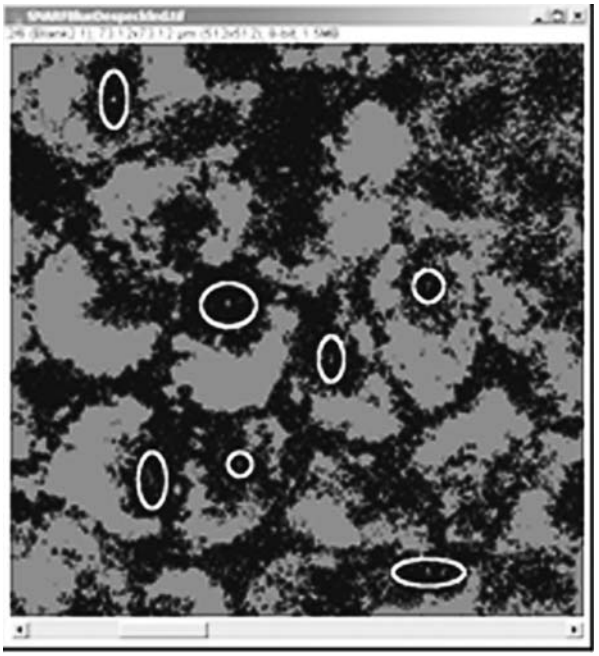

Fig. 17.15. ROIs selection for cytosol under nucleus areas on blank cells (SNARF-1_{590} channel). Each individual ROI in the composite image is numbered. This identification number allows retrieval of ROI statistics from the ROI export list feature in ImageJ.

ate extension number. Check if the Composite.roi applies to all the images in the stack. Due to cell movement, each image should be checked individually, and the position of the ROIs adjusted, to avoid any "contamination" with mitochondrial pixels. Save the adjusted ROI composite for each image in a separate file. Use Measure in RoiManager to calculate the averaged value for the pixels inside the selected ROIs for each image in the stack (i.e., cytosol beneath the nucleus).The background autofluorescence values obtained for our measurements, based on the above protocols, are presented in **Fig. 17.16**.

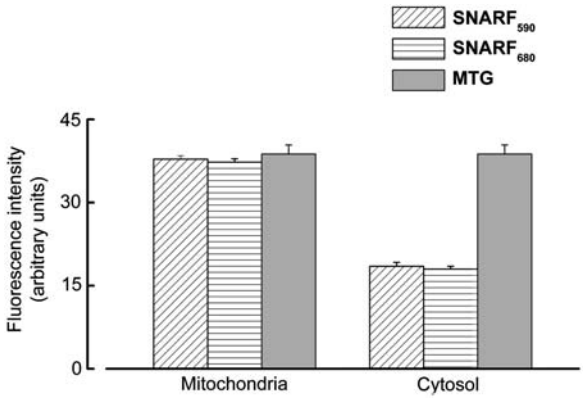

Fig. 17.16. Autofluorescence levels for mitochondria and cytosol. Autofluorescence was measured in the corresponding channels for SNARF-1_{590}, SNARF-1_{680}, and MTG based on the distinct pattern of mitochondrial and nuclear areas for unstained MDCK monolayers. Mean ± SE (N=6). Detector gain 1100 (Zeiss software settings). Reproduced with permission from *Kidney Int* (3).

Another way of calculating the background autofluorescence for mitochondrial area and cytosol beneath the nucleus, respectively, relies on the observation that there is no crosstalk between the MTG and SNARF-1 channels (**Fig. 17.7**). Therefore, by performing three multi-track measurements on cells loaded only with MTG, it is possible to create a very precise mask of the pixels related to mitochondria and the pixels beneath the nucleus, free of any mitochondrial contribution. Applying this mask on both SNARF-1_{680} and SNARF-1_{590} stacks will provide the background values for the mitochondria and cytosolic regions, respectively, during the entire measurement. This procedure is identical with the ones explained previously in **Sections 3.5.2** and **3.5.3**, respectively.

3.5.5. Selection of Pixels Containing Mitochondrial Na^+ Information Based on CoroNa Red and MTG Processing

The CoroNa Red fluorescence has to be corrected for non-mitochondrial CoroNa Red fluorescence, including the weak cytosolic CoroNa Red staining and the pronounced staining of

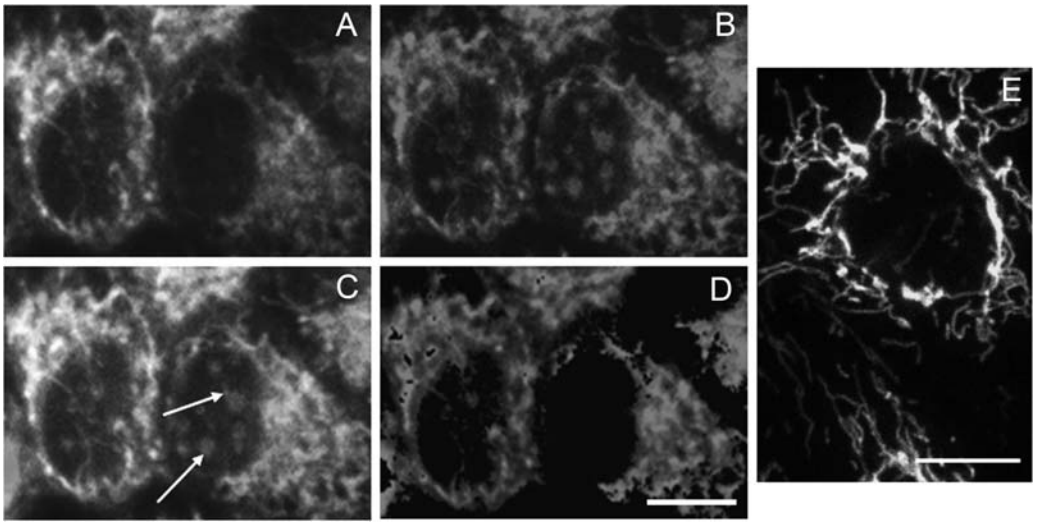

Fig. 17.17. Confocal images of MDCK cells loaded with MitoTracker Green (MTG) and CoroNa Red (**a**–**d**) and cells only loaded with MTG (**e**). MTG (**a**) and CoroNa Red (**b**) staining of mitochondria in MDCK cells. The staining with the Na^+-sensitive probe CoroNa Red was spatially correlated with the mitochondrial marker MTG (**c**), except for a weak CoroNa Red staining of the cytosol and a more pronounced staining of nuclear structures, presumably nucleoli (*arrows*). Application of the "mask" procedure (for details *see* **Section 3.5.5**) yielded an image consisting of only mitochondrial CoroNa Red fluorescence intensities (**d**) (scale bar=10 μm). (**e**) Mitochondrial staining in cells showing an extensive dynamic mitochondrial network under control conditions. Only weak rhod 2 staining of the cytosol (data shown in (5)) was observed and pronounced staining of nuclear structures similar to (**c**). Scale bar = 10 μm. (**a**–**d**) Reproduced with permission from *J Am Soc Nephrol* 2005 (4). (**e**) Reproduced with permission from the *Am J Physiol Renal Physiol* (5).

structures within the nuclei, presumably nucleoli (indicated by arrows in **Fig. 17.17c**). An MTG masking procedure was developed to retrieve only the mitochondrial CoroNa Red fluorescence intensity from the measured data (**Fig. 17.17d**).

1. Data collection in brief. Sets of multitrack images are collected: a CoroNa Red, followed by an MTG image under published conditions. Three multitrack images are collected for CoroNa Red at every time point to establish an average. An image set was collected every 3 min, for 1 h, since the dye proved to be very stable. Focus was readjusted when required.
2. Convert and export raw image data into uncompressed.tif. Split the multitrack.lsm confocal microscope images with Zeiss data collection software or use the LSM Toolbox in ImageJ. Put .tif converted CoroNa Red and MTG images with a sequence number in the filename in separate folders. ImageJ possesses convenient features, e.g., loading an entire stack upon selecting the first file in a folder. Using the File\Import\Image sequence feature in ImageJ image stacks are imported. Save as raw data MTGStack.tif and CoroNaRedStack.tif 8-bit (numerical values between 0 and

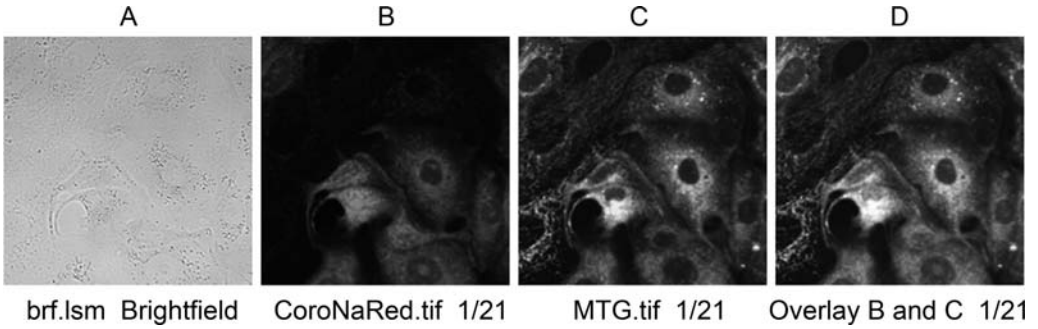

Fig. 17.18. Raw transmission and fluorescence images of MDCK cells loaded with CoroNa Red and MTG.

255) and as a merged StackRGB.tif for a color representation (**Fig. 17.18b–d**).

3. Despeckle raw image stacks.
4. Eliminate saturated pixels both for MTG (always required) and CoroNa Red (hardly ever). Set threshold to 255 numerical value. Process\Binary\Convert to Mask and Invert. Divide by 255 and multiply the mask with images.
5. Subtract autofluorescence of support microscope slide and buffer solution when required. Background autofluorescence intensity from mostly the glass support and maybe buffer solution contribution was always at most 16 or 17 as determined from the pixels with the lowest signal. These numbers were checked also on unstained and single-dye stained cells on a regular basis and after each new cell passage number. Save StackMaskSatBkgndCorrected and StackCoroNa RedSatBkgndCorrected image sets.
6. MTG "mask" creation. For StackMaskSatBkgndCorrected.tif select best rather high threshold 70à 85–200 with a strong mitochondrial contribution. Adjust threshold. Click Apply to convert to binary and divide by 255. Save as StackMask.tif (**Fig. 17.19a**) with numerical value one for mask pixels to be retained and zero otherwise (pixels not to be used). This includes pixels set to zero for accidental saturation, although the instrument settings used avoided this situation in general as much as possible.
7. CoroNa Red: retrieval of MTG mask related pixels. Multiply StackMask.tif with StackCoronaRedSatBkgndCorrected.tif. Save as Result.tif stack into AnalysisExp01 folder, for example (**Fig. 17.19b, c**). Note the differences in MTG area and the perinuclear location of saturated pixels regions in C as compared with B.
8. ROI selection. Open the Result.tif and StackMask.tif stacks. Select five (5) separate ROI areas on the first Result image (write down X, Y, W, H coordinates) (**Fig. 17.19d**).

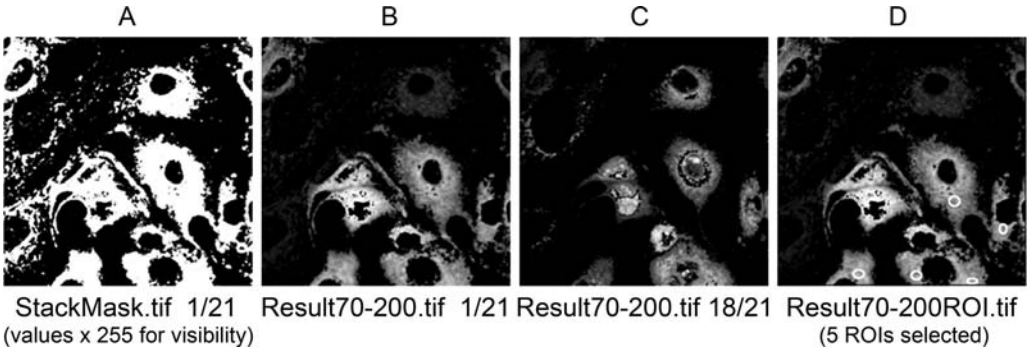

Fig. 17.19. MTG mask creation and retrieval of CoroNa Red mask images. (**a**) Binary MTG mask (×255 for visibility). A rather high threshold level ranging from 70 to 200 ensures selection of pixels with a strong mitochondrial contribution. (**b**, **c**) Masks applied to CoroNa Red images. Differences in the extend of saturated pixels in the perinuclear regions of 1/21 (**c**) as compared with 18/21 (**b**) due to contraction over time of the mitochondrial network. The notation *n/m* refers to the *n*th image in a stack comprising *m* images. (**d**) Selection of five separate ROI areas on the first result image (1/21). Bright areas are avoided altogether. Due to cellular motility and the requirement of validity over the whole stack, sizes of individual ROIs are small.

Use ROI manager. Avoid very bright areas. Check that each created ROI properly covers intended cellular areas over the whole image stack in order to avoid lacking or wrong area data due to cell motion.

For bleach correction and result normalization select StackMask.tif stack and Edit\Restore selection (ROI is transferred).

Create a *z*-axis intensity profile table via Image\Stacks\Plot Z-axis profile of StackMask.tif.

In the Result window: Edit\Copy All.

Paste the data from StackMask, Result.tif windows, and ROI summed intensity values as well as the ROI areas selected into Excel ∗.xls files.

9. Excel and Origin statistical analysis. Create three separate Excel sheets.

10. ROI normalisation procedure. Due to contraction of the mitochondrial network near the end of a MI experiment MTG image, areas may start to saturate. Saturated pixels are set to zero and are eliminated. The obtained CoroNa Red and rhod 2 fluorescence values for the ROIs were normalized with regard to the number of pixels with a mask value of one in the mask area to compensate for differences in mitochondrial density in each ROI of subsequent images in the stack. **Figure 17.20** shows an enlarged region of the ROI in the lower right corner of **Fig. 17.19d**.

DataROI 1 (Raw *z*-axis intensity profile data). To be stored for both the MTG and CoroNa Red sets of, for example, five ROIs for each image in the stacks.

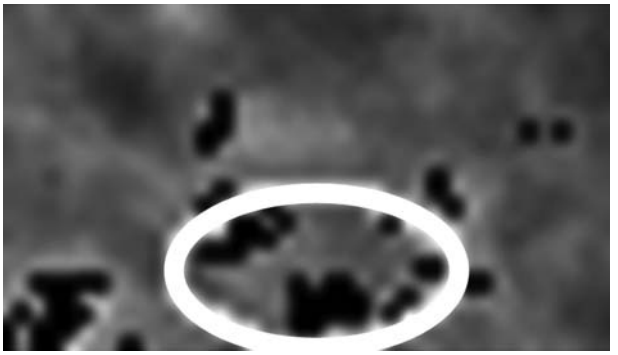

Fig. 17.20. Enlarged ROI showing MTG saturated pixels set to zero. Enlarged region around the ROI in the lower right corner of **Fig. 17.19d**.

SheetROI 1 (final table with averaged values + normalized percentages + error analysis).

3.5.6. Selection of Pixels Containing Mitochondrial Ca^{2+} Information Based on Rhod 2 and MTG Processing

Identical to the CoroNa Red protocol presented in **Section 3.5.5**. To minimize as much as possible the photobleaching of rhod 2, a multi-track series (consisting of one MTG image and one rhod 2 image) was collected every 20 min during 1 h. Focus was readjusted when required.

3.6. In Situ Dye Calibration Protocols

3.6.1. In Situ pH Calibration of SNARF-1

Given the fast bleaching of SNARF-1, it is not possible to perform the calibration at the end of each experiment, but this is done in separate measurements. Calibration of the ratio of the fluorescence signals from SNARF-1 is performed according to the method of Thomas et al. (9).

1. Load the cells with SNARF-1 in the cytosol and with SNARF-1 plus MTG in mitochondria, according to Protocol 2 (**Section 3.3.1**).
2. Prepare a solution of high-K^+ (**Section 2.3.2**) containing also 13 μM nigericin and 1 μM FCCP (to equilibrate the H^+ gradient across the plasma and mitochondria membrane, respectively) and 20 μg/ml oligomycin to inhibit the mitochondrial F_1F_0-ATPase.
3. Set the pH of this solution to four different values in the range of 6.8–7.8. The exact pH of each solution at 37°C should be recorded.
4. Place the holder containing the monolayer on the microscope stage. Remove the NSS medium from the cells and add the first pH calibrating solution. Allow 20 min for equilibration before measuring each pH point. When changing the pH calibration solutions, gently wash cells twice with the new pH solution to be measured.

5. To ensure that pH equilibration reached a steady state, each calibration point was measured after 20 and 30 min, respectively, of equilibration. At both time points the measured pH values were similar.
6. To avoid any possible systematic errors, perform the calibration procedure in both directions, from low to high pH and vice versa.
7. Following the mitochondrial "MTG mask" analysis, plot the calibration solution pH versus the SNARF-1 ratio in the cytosol and in the mitochondria, respectively, for all four pH points. Perform linear regression on the line obtained in each case to determine the slope (multiplier) and the *y*-intercept. Use these values to perform a linear scaling of the SNARF-1 fluorescence ratio.

The result of SNARF-1 calibration in living MDCK cells following the presented protocol are illustrated in **Fig. 17.21**.

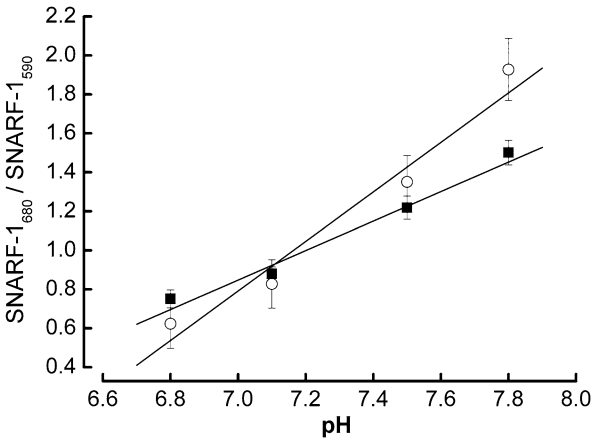

Fig. 17.21. pH calibration for the SNARF-1 signal. Averaged SNARF-1 ratios (680/590 nm) for cytosol (○) and mitochondria (■) were plotted against the pH of the bathing solution. *Error bars* indicate the SEM on the SNARF-1 ratio averaged over five experiments. Reproduced with permission from *Kidney Int* (3).

3.6.2. In Situ $[Na^+]_m$ Calibration Protocol for CoroNa Red

1. Expose the cells to various extracellular Na^+ concentrations in the presence of 10 μM gramicidin D, 10 μM nigericin, 20 μM monensin, 1 μM FCCP, and additionally 20 μg/ml oligomycin (*see* **Note 17**). Allow 15 min of equilibration before measuring each $[Na^+]$ point.
2. The solutions with various sodium concentrations were prepared by mixing in different proportions the two calibration solutions (**Section 2.3.3**) of equal ionic strength and osmolality. The sodium concentration of the solution was set to five different values in the range of 145 to 0 mM (145, 120, 72.5, 60, and 0). The plot of the normalized fluorescence

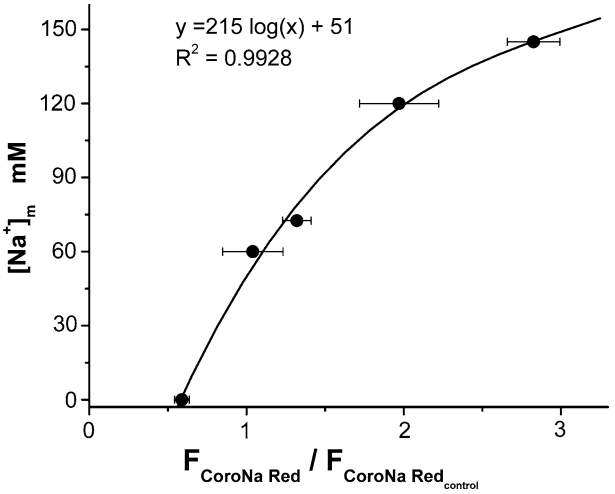

Fig. 17.22. In vivo calibration curve of the mitochondrial CoroNa Red signal in MDCK cells (4). Mitochondrial Na^+ concentration ($[Na^+]_m$) as a function of the fluorescence intensity of the normalized CoroNa Red signal (N=7) ± SE (standard error). The control CoroNa Red fluorescence intensity is defined as the fluorescence intensity in normal, untreated MDCK cells after loading with CoroNa Red. Reproduced with permission from *J Am Soc Nephrol* 2005 (4).

intensity of CoroNa Red against $[Na^+]_m$ resulted in a logarithmic curve (**Fig. 17.22**).

3. Since CoroNa Red is not a ratiometric probe, non-Na^+-dependent changes in the mitochondrial CoroNa Red fluorescence, e.g., changes induced by shrinkage or swelling of mitochondria, might lead to misinterpretation of the results. For assessing the contribution of non-specific changes in mitochondrial CoroNa Red fluorescence intensities, the CoroNa Red_{mito}/MTG fluorescence ratio was used to calculate $[Na^+]_m$. Because changes in the mitochondrial volume induce equal relative changes in the fluorescence of both mitochondrial CoroNa Red and MTG, the CoroNa Red_{mito}/MTG ratio is expected to be volume independent. The $[Na^+]_m$ values obtained by the "CoroNa Red_{mito}/MTG fluorescence ratio" method or calculated directly from the mitochondrial CoroNa Red fluorescence intensities are not significantly different. Therefore, the latter method is applied to calculate $[Na^+]_m$.

3.6.3. No Calibration Protocol for Rhod 2

Calibration was not performed in rhod 2 experiments. Only *relative* changes in mitochondrial rhod 2 fluorescence as induced by treatment of the cells with metabolic inhibitors were assessed. The observed relative increase in mitochondrial rhod 2 fluorescence during MI is underestimated because signal is lost throughout the 60 min protocol. This loss of signal might be ascribed to either

photobleaching of the probe or leakage of the rhod 2 dye out of the mitochondrial matrix. Observed changes were not related to focus drift of the instrument since the focus was re-optimized before every image collection.

4. Notes

1. Fluorescence dye solutions have to be protected from light.
2. When removed from the freezer, allow the aliquots to equilibrate to room temperature in the dark (aluminum foil wrapped). This will prevent the contamination of DMSO with water (as is the case when a bottle is opened before the content has warmed sufficiently to room temperature).
3. Unless stated otherwise all solutions should be prepared in water that has a resistance of 18.2 MΩ; this standard is referred to as "water" in this text.
4. All chemicals are analytical grade.
5. All solutions can be stored at 4°C for about 1 month (check regularly that fungi do not appear in them).
6. The recommended seeding density allows tight confluent monolayers of MDCK cells to be obtained after 3 days of culturing, as well as an increased stability of the cells on the glass surface. For other cell types the seeding density should be adjusted accordingly.
7. At higher passage numbers we observed a delay in cell growth, the confluency being reached only after 5 days in culture. Moreover, the monolayer became less uniform, the morphology of the cells changing from flat, "polygonal" shape, to a more rounded shape. This change in morphology observed for older passages is illustrated in **Fig. 17.1**. We noticed that when the passage number was high, growth to confluency was slow and patchy with in general fuzzy small rounded cells. Switching to new low passage numbers remedied all issues.
8. On a regular monthly basis potential mycoplasma contamination should be checked with, e.g., the mycoplasma PCR ELISA kit from Roche (cat no 11 663 925 910) (Vilvoorde, Belgium).
9. Washing gently means avoiding direct contact with any cell covered areas, not hitting attached cells head-on with a syringe flow but breaking the flow by very gently squishing against the walls of the cell holder. Each wash is performed with 2 ml buffer, letting it sit for 30 s. Use very

gentle re-suction, keeping the needle tip as far away from the cell covered surfaces and maintaining a low liquid flow.

10. The second loading protocol was developed based on the observation that during the experimental time course the cytosolic fluorescence intensity is decreasing continuously due to a gradual loading of the mitochondria. Therefore, to be able to work with a sufficiently high signal-to-noise ratio of SNARF-1 in the cytosol during longer time periods, the mitochondrial "sink" was loaded first, followed by a second loading of the cytosolic pool with SNARF-1.
11. When dual labeling is used, the pinhole size has to be adjusted for each channel in such a way that the same observed optical slice thickness is observed for all emission channels.
12. This step is very important for the reliability of the method, as using the averaged autofluorescence intensity over the whole cell can induce large errors in the calculated values for pH_i and pH_m. This will affect mainly the data from the final part of the experiments, when SNARF-1 intensity is lowered due to photobleaching (see below) and dye leakage, and therefore the contribution of the background to the calculations becomes substantial.
13. As discussed in **Section 3.4.1**, one concern raised by repeated laser illumination on living cells is related to the phototoxicity which might occur. Previous phototoxicity studies (10, 11) have shown that cellular stress induced by laser excitation in the visible range (as applied in our experimental protocol) can be detected via an increase in the cellular autofluorescence. Monitoring changes in autofluorescence during the experimental protocol can therefore be a useful method to study phototoxicity.
14. These settings allowed us to perform the following protocol with minimal light exposure and photobleaching in order to monitor the pH_i and pH_m changes in MDCK cells exposed to MI: we first acquired two pre-MI control images, followed by SNARF-1 ratio imaging at 5, 10, 20, 40, and 60 min during MI. After replacing the MI solution by fresh NSS, the SNARF-1 ratio was again measured after 15 and 30 min into the recovery period of the cells.
15. Mitochondrial and cytosolic regions of interest should be carefully selected since at the given pinhole opening (**Section 3.4.2**) the optical slice volume contained both cytoplasmic and mitochondrial localized fluorescence information. Just taking the average of all pixels (related to both mitochondrial and cytosolic signals) is completely

erroneous and incorrect since the background signal levels differ between the two. To properly create the MTG mask for either the pixels under the nucleus (lack of any MTG signal) or the mitochondria-related pixels (maximum MTG signal), the MTG image stack was enhanced and stretched in order to observe even the weakest observable signal.

16. It is to be understood that this part is not easy to automate. Due to cellular motion usually none of the selected ROI areas carries over to the next image and the whole process has to be repeated separately for each image in the stack.
17. Calibration is done starting from high concentration to zero.

Acknowledgments

The authors acknowledge Mr. J. Janssen for his excellent technical assistance with the cell culture. We also thank Mrs. R. Beenaerts, Mr. W. Leyssens, Mr. P. Pirotte, and Mr. R. Van Werde for their technical help and Mrs. M. Ieven for artwork. We are also grateful to various groups for the free software for confocal image analysis: LSM Toolbox plug-in (University of Strasbourg, Strasbourg, France; Dr. J. Mutterer, Dr. Y. Krempp, and Dr. P. Pirrotte), ImageJ (NIH, Bethesda, MD; Dr. W. Rasband; available online: http://rsb.info.nih.gov/ij/plugins/lsm-reader.html), and VolumeJ (Utrecht University, Utrecht, the Netherlands; Dr. M. Abramoff).

This work was supported by a bilateral research collaboration program between Flanders and Hungary (BIL01/18 HON), between Flanders and Romania (BOF 05 B03), and by the Research Foundation Flanders (FWO, GO270.07). Support by IAP P6/27 *Functional Supramolecular Systems* (BELSPO) and by the FWO-onderzoeksgemeenschap *Scanning and Wide Field Microscopy of (Bio)-organic Systems* are also thankfully acknowledged.

References

1. Sekine, T., Miyazaki, H., Endou, H. (2008) Solute transport, energy consumption and production in the kidney, in Seldin and Giebisch's, in *The Kidney, Physiology and Pathophysiology, vol. I,* (Alpern, R.J., Hebert, S.C., eds.), Academic Press, Elsevier Inc: Burlington, MA. pp. 185–210.
2. Schrier, R.W. (2003) Acute renal failure: pathogenesis, diagnosis and management, in *Renal and Electrolyte Disorders* (Schrier, R.W., ed.), 6th Edition, Lippincott Williams & Wilkins: Philadelphia, pp. 401–455.
3. Balut, C., vandeVen, M., Despa, S., Lambrichts, I., Ameloot, M., Steels, P., Smets, I. (2008) Measurement of cytosolic and mitochondrial pH in living cells during reversible

metabolic inhibition. *Kidney Int*, **73**, 226–232.
4. Baron, S., Caplanusi, A., vandeVen, M., Radu, M., Despa, S., Lambrichts, I., Ameloot, M., Steels, P., Smets, I. (2005) Role of mitochondrial Na^+ concentration, measured by CoroNa red, in the protection of metabolically inhibited MDCK cells. *J Am Soc Nephrol*, **16**, 3490–3497.
5. Smets, I., Caplanusi, A., Despa, S., Molnar, Z., Radu, M., vandeVen, M., Ameloot, M., Steels, P. (2004) Ca^{2+} uptake in mitochondria occurs via the reverse action of the Na^+/Ca^{2+} exchanger in metabolically inhibited MDCK cells. *Am J Physiol Renal Physiol*, **286**, F784–F794.
6. Tsien, R.Y., (1981) A non-disruptive technique for loading calcium buffers and indicators into cells. *Nature*, **290**, 527–528.
7. Takahashi, A., Zhang, Y., Centonze, E., Herman, B. (2001) Measurement of mitochondrial pH in situ. *Biotechniques*, **30**, 804-808, 810, 812 passim.
8. Despa, S., (2000) *Microfluorimetry of Epithelial Cells: Lifetime-Based Sensing of Na^+ Concentration and the Effects of Chemical Hypoxia*, Physiology Department, Hasselt University: Diepenbeek (Royal Library Albert I, Brussels, D-2000-2451-6), p. 18.
9. Thomas, J.A., Buchsbaum, R.N, Zimniak, A., Racker, E. (1979) Intracellular pH measurements in Ehrlich ascites tumor cells utilizing spectroscopic probes generated in situ. *Biochemistry*, **18**, 2210–2218.
10. Dailey, M.E., Manders, E., Soll, D., Terasaki, M., (2006) Confocal microscopy of living cells, in *Handbook of Biological Confocal Microscopy*, (Pawley, J.B., ed.), 3rd Edition, Springer Science + Business Media, LLC: New York, pp. 381–403.
11. König, K., (2001) Cellular response to laser radiation in fluorescence microscopes, in *Methods in Cellular Imaging*, (Periasamy, A., ed.), Oxford University Press: Oxford, pp. 236–251.